Available online at www.sciencedirect.com
SCIENCE DIRECT®
Journal of Solid State Chemistry 177 (2004) 4588–4596
JOURNAL OF SOLID STATE CHEMISTRY
www.elsevier.com/locate/jssc

Selective synthesis of $CdWO_4$ short nanorods and nanofibers and their self-assembly

Hai-Lin Wang, Xiao-Dong Ma, Xue-Feng Qian*, Jie Yin, Zi-Kang Zhu

State Key Laboratory of Composite Materials, School of Chemistry and Chemical Technology, Shanghai Jiao Tong University, Dongchuan Road, Shanghai 200240, People's Republic of China

Received 24 July 2004; received in revised form 7 September 2004; accepted 14 September 2004
Available online 11 November 2004

Abstract

Single-crystalline $CdWO_4$ nanorods and nanofibers are selectively prepared based on hydrothermal treatment with cetyltrimethylammonium bromide (CTAB) as capping molecule and ordinary inorganic reactant as precursors through exactly controlling the pre-treated condition. With almost uniform breadth and pointed ends, the obtained short nanorods show a relatively thick nature along [010] direction and self-assemble to an ordered structure with (001) and (010) faces, respectively, while the as-prepared nanofibers are flexible and vertically self-assemble to form woven network. The mechanism of selective preparation and self-assembly was also discussed. Both obtained nanorods and nanofibers display a very strong blue-green luminescence property at room temperature.

Keywords: Cadmium tungstate; Nanorod; Nanofiber; Self-assembly

1. Introduction

Recently, the synthesis and fabrication of one-dimensional (1D) nanosized materials have attracted great interest because of their distinctive and outstanding properties, and potential applications in nanodevices. A considerable variety of 1D nanostructures, such as metals, metal oxides, metal salts, hydroxides, sulfides, and other semiconductors with nanorod, nanowire, nanoribbon, nanotube and nanobelt morphologies, have been synthesized by many kinds of methods and techniques during the past decade, which enrich the "nanobox" that is essential for the "bottom-up" approach in nanoscience and nanotechnology [1–6]. A fundamental step for this approach is assembly of these 1D nanostructures to a two-dimensional (2D) framework, and many examples of the formation of inorganic 2D arrays and structures by solution route have been reported in recent years. For instance, the self-assembly of FeOOH [7], $BaCrO_4$ [8,9], CdSe [10], Ag [11,12] and Au [13] nanorods or nanowires to 2D and 3D spontaneous superlattices has been observed. Though much improvement has been made in the synthesis of 1D nanosized materials, it is still a challenge to seek out a convenient solution route for controlled preparing of 1D nanostructures and their assembly.

Cadmium tungstate ($CdWO_4$) is considered to be an attractive material because of its optical, chemical and structural properties. It is well known that $CdWO_4$ crystals with monoclinic wolframite structures have high thermal stability, high average refractive index, low radiation damage, low intrinsic background, low afterglow, and high X-ray absorption, and they can be used in spectrometry and radiometry of radionuclide in extra-low activities. Furthermore, the crystal thickness to stop 150 keV photons is only 3 mm due to the high density of $CdWO_4$, so the high stopping power and the low afterglow of $CdWO_4$, together with the possibility to

*Corresponding author. Fax: +86 21 5474 1297.
E-mail address: xfqian@sjtu.edu.cn (X.-F. Qian).

0022-4596/$ - see front matter © 2004 Elsevier Inc. All rights reserved.
doi:10.1016/j.jssc.2004.09.012

detect the scintillation light efficiently with photodiodes, make it an attractive scintillator for high-energy nuclear spectroscopy and X-ray detection (e.g., in CT scanners) [14–17].

Single crystalline $CdWO_4$ is desired for the above applications because the light scattering at grain boundaries makes polycrystalline $CdWO_4$ ceramics unsuitable to those applications. Conventionally, single crystalline $CdWO_4$ can be prepared through the Czocharalski method at high temperature. And pulsed laser ablation [18], spray pyrolysis [19] and sol–gel process [20] are also reported to prepare $CdWO_4$ thin films. Recently, the solution chemical method has been considered to be a promising option due to its simple, fast, less expensive virtues and the diversity of reactions. To date, the procedures that have been reported to prepare nanostructured $CdWO_4$ in solution were mainly a hydrothermal process to $CdWO_4$ nanorods [21], a polymer-controlled route to 1D and 2D very thin nanocrystals [22] and a route using lamellar inorganic-surfactant precursors to synthesize $CdWO_4$ nanowires [23].

Though the morphologies of $CdWO_4$ nanomaterials can be controlled by the double-hydrophilic block copolymers or through lamellar inorganic-surfactant precursors, cetyltrimethylammonium bromide (CTAB), which is one of the most common surfactants and has been proved to be quite an effective capped agent for the growth of the semiconductors or other compounds [24], has not been directly used to control the morphology of $CdWO_4$. Herein, we report a convenient aqueous solution route based on the hydrothermal process with the help of CTAB to selectively prepare single crystalline $CdWO_4$ nanorods and nanofibers through the accurate control of the pre-treated condition. Moreover, self-assembly was observed in both $CdWO_4$ nanorods and nanofibers. The formation mechanism is also discussed here.

2. Experimental section

2.1. Materials

Analytical grade sodium tungstate ($Na_2WO_4 \cdot 2H_2O$), cadmium chloride ($CdCl_2 \cdot 2.5H_2O$) and CTAB were purchased from the Shanghai Chemical Reagent Company and used as received without further purification. The reaction was carried out in a 30 mL capacity Teflon-lined stainless steel autoclave in a digital-type temperature-controlled oven.

2.2. Preparation

In a typical procedure, 0.9 mmol of $Na_2WO_4 \cdot 2H_2O$, 0.9 mmol $CdCl_2 \cdot 2.5H_2O$ and 1.8 mmol of CTAB were dissolved in 25.0 mL of deionized water to prepare $CdWO_4$.

$CdWO_4$ nanorods and nanofibers are selectively prepared through exactly controlling the pre-treated condition. To prepare $CdWO_4$ short nanorods, $CdCl_2 \cdot 2.5H_2O$ was added to the Na_2WO_4 solution with CTAB at the same time and vigorously stirred for 30 min to form a mixture containing amorphous particles. The resulting precursor suspension was transferred into a Teflon-lined stainless steel autoclave, then sealed and maintained at 150 °C for 12 h. To prepare $CdWO_4$ nanofibers, the same reaction time and temperature were maintained. The only difference was that Na_2WO_4 and CTAB were first dissolved in deionized water without $CdCl_2$. After being stirred for 30 min, a homogeneous solution was formed and directly loaded to the autoclave. Then 0.9 mmol $CdCl_2 \cdot 2.5H_2O$ was slowly added to the autoclave with minimal disturbance (Scheme 1), and maintained at 150 °C for 12 h.

After reaction, the autoclaves were cooled to room temperature naturally. The products were filtered, washed several times with deionized water and absolute ethanol to remove surfactants and other impurities, and then dried in vacuum at 60 °C for 4 h.

2.3. Characterization

The phase identification was carried out using powder X-ray diffraction (XRD, Shimadzu XRD-6000) with

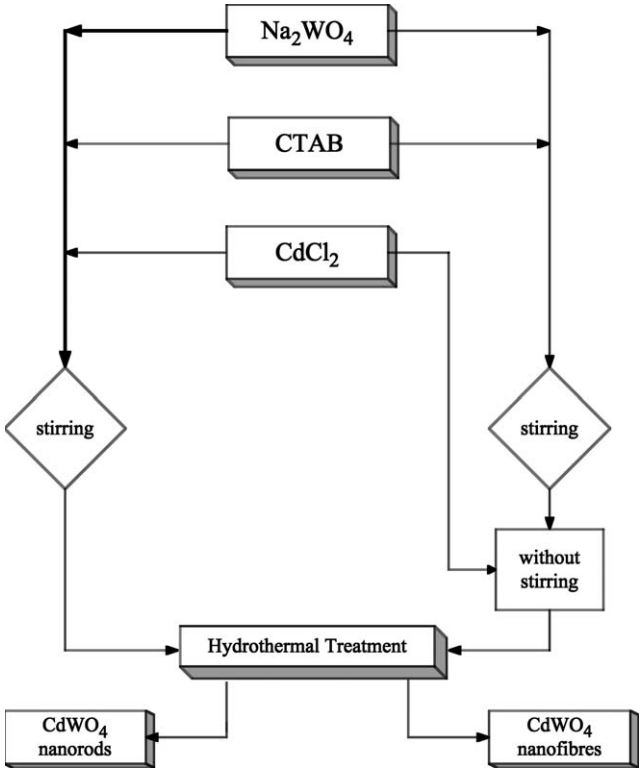

Scheme 1. Selected control strategy for $CdWO_4$ nanorods and nanofibers.

Cu$K\alpha$1 radiation ($\lambda = 1.5406$ Å) 2θ from 10° to 70° at a scanning rate of 4°/min. X-ray tube voltage and current were set at 40 kV and 30 mA, respectively. The observation of morphology and selective area electron diffractions (SAED) of the samples were carried out using a transmission electron microscope (TEM, JEOL JEM-100CX). The electron beam accelerating voltage was set at 100 kV. The solid sample was first suspended in absolute ethanol by ultrasonic treatment for 20 min. A drop of this well-dispersed suspension was then trickled on a piece of carbon-coated copper grid. Before being placed into the TEM specimen holder, the copper grid was air-dried under ambient conditions. The photoluminescence (PL) of the sample was investigated on Perkin Elmer Luminescence Spectrometer LS50B at room temperature.

3. Results and discussion

3.1. Crystalline analysis

Fig. 1 is the representative XRD pattern of samples, in which all the peaks located at 2θ values of 10–70° correspond to the characteristic diffractions of monoclinic phase $CdWO_4$ with lattice constants $a = 5.03$ Å, $b = 5.86$ Å, $c = 5.07$ Å and $\beta = 91.47$ (JCPDS card No.14-676). It verifies that the $CdWO_4$ products are phase pure and well crystallized. The difference in shape and intensity between the diffraction peaks of $CdWO_4$ nanorods and nanofibers indicates some differently orientated growth between them. The sharper and stronger nature of nanorod diffraction peaks in 0 1 0 and 0 2 0 plane compared with that of standard pattern (Fig. 1c) and nanofiber patterns suggests possible relatively preferential orientation along [010] direction.

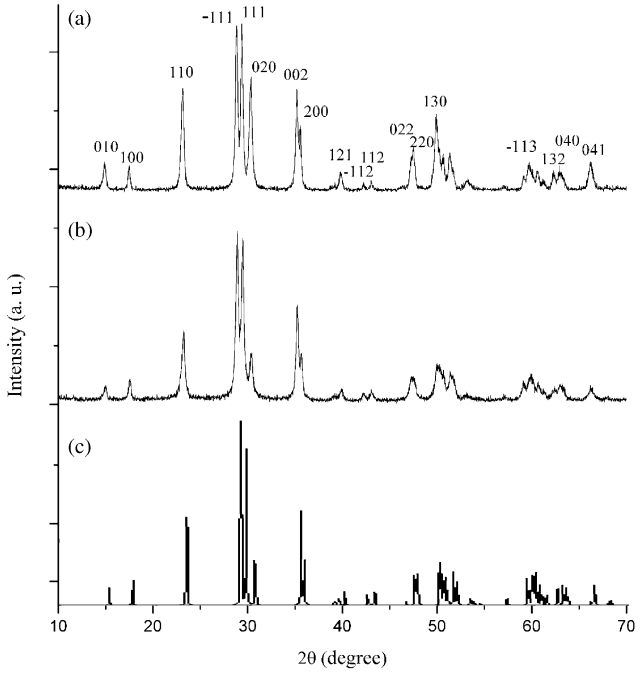

Fig. 1. XRD pattern of the as synthesized $CdWO_4$: (a) nanorods; (b) nanofibers; and (c) JCPDS card No. 14–676. Both of the products were obtained by hydrothermal treatment at 150 °C for 12 h.

3.2. Morphologies observation

As shown in TEM images (Figs. 2a and b), the obtained $CdWO_4$ nanocrystallites appear to have uniform rod-like morphologies with pointed ends, and have widths of 20–40 nm, lengths of 80–150 nm and an aspect ratio of about 4–6. It is obvious that these short rods show comparatively thicker nature than that which has been reported recently [21,22]. In general, $CdWO_4$ easily forms relatively thin structures due to its intrinsic (010) cleave plane because of the chain structure of the W octahedra in the wolframite type structure. So we think that the thick nature of $CdWO_4$ obtained in our approach is mainly caused by the effect of CTAB. The SAED pattern of $CdWO_4$ short nanorods (Fig. 2c), which can be indexed to [010] zone spots, shows the single crystalline structure of the rods. Based on the results of SAED, it is known that the preferred growth direction of these rods is [100] and has a relative thick nature along *b*-axis (Scheme 2a and b). When the reaction time was increased to 24 h, the morphologies of these nanorods did not change obviously. Though some rods prolong in length, they almost do not increase in widths (Figs. 2d and e).

As can be seen in the TEM images (Figs. 2a, d and e), most of the short nanorods can self-assemble to ordered structures and few isolated rods were observed. The assembled structure are constructed by several rods

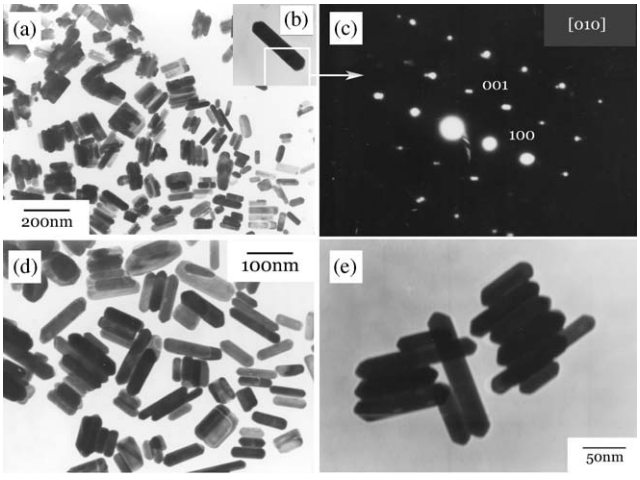

Fig. 2. Representative TEM images for $CdWO_4$ nanorods treated under hydrothermal process for: (a) 12 h and (d), (e) 24 h; (b) a single nanorod and (c) SAED of a single rod.

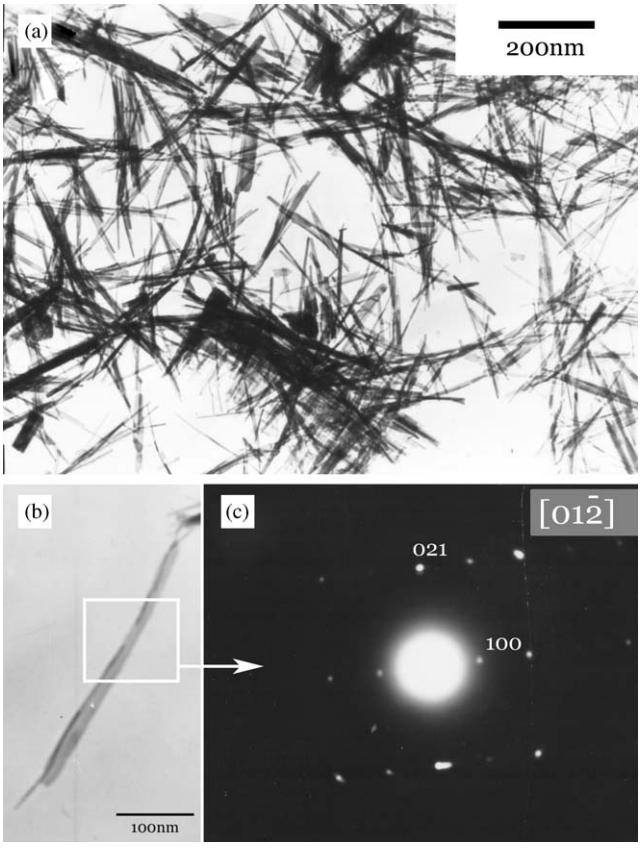

Fig. 3. Representative TEM image of the nanofibers (a); a single nanofiber (b) and its ED (c).

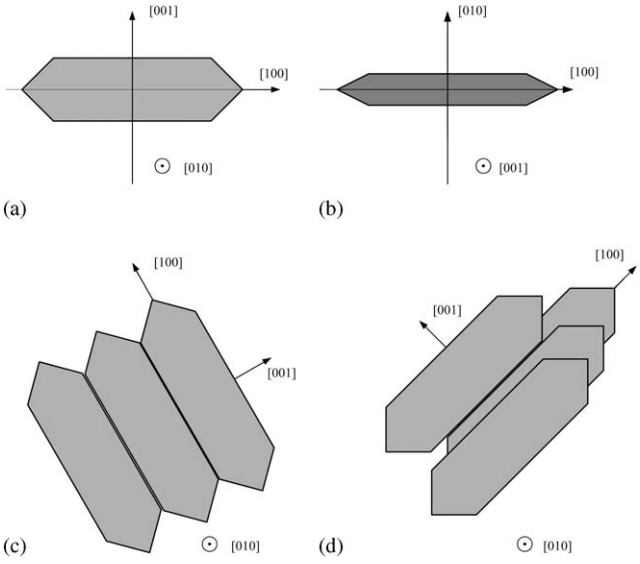

Scheme 2. Schematic illustration of the nanorods (a, b) and their self-assembly (c, d). The symbol "⊙" denotes a direction vertically outside the paper plane.

attaching with their (001) or (010) planes, respectively (Schemes 2c and d), and the maximal assembled structure includes more than ten nanorods. It is noted that most of the assembling rods have similar widths. The morphologies and assembly phenomenon of the nanorods are quite similar to what has been reported by Zeng, etc. about CuO [25]; nevertheless the growth direction is different and the attachment of surfaces on the pointed ends have seldom been observed in our work. Thus, the nanorods do not self-assemble to network structure.

Fig. 3a shows the representative morphologies of as-prepared $CdWO_4$ nanofibers. From the TEM image, we can see that these nanofibers have a relatively thin nature and higher aspect ratio with widths from one to several decade nanometers and lengths from several hundred nanometers to several micrometers. From this we can also find that many nanofibers curve, which indicates that the obtained $CdWO_4$ nanofibers are flexible and quite different from the obtained $CdWO_4$ nanorods. Fig. 3c is SAED of a single nanofiber (Fig. 3b), which can be indexed to [01$\bar{2}$] zone spots. Therefore, the preferred growth orientation of these nanofibers is still in [100] direction.

The self-assembly of these nanofibers is also discovered in the samples. The nanofibers are self-assembled perpendicularly together to form nets or web structures (Fig. 3a). In such an area of Fig. 4a, several pieces of this nanonetwork can be found, which indicate that this assembly phenomenon is not occasional or just caused by the random aggregation of nanofibers in the procedure of TEM sample preparation. Figs. 4b and c show a piece of well-assembled $CdWO_4$ network nanostructure. From the magnified image (Fig. 4d), the detailed construction of the assembled $CdWO_4$ can be observed. To the best of our knowledge, this kind of the woven intertexture has not been prepared in solution route before. The SAED pattern of the network structure (Fig. 4e) indicates that the structure is well crystallized and regularly organized by the nanofibers. The pattern can be considered as a combination of two mutually perpendicular ED patterns of $CdWO_4$ nanofibers indexed to [01$\bar{2}$] zone sports. This result further proves that the network structure is assembled by mutually perpendicular $CdWO_4$ nanofibers.

3.3. Mechanism discussion

The mechanism of this selective synthesis is not very clear yet; however we believe that CTAB plays a critical role in this reaction system because the selective preparation cannot be realized under hydrothermal condition without the presence of CTAB. Considering that a highly supersaturated solution was adopted as preparation medium and the precursor is amorphous fine particles, this reaction system is still a typical hydrothermal ripening procedure based on the well-known "Ostwald ripening process" [26]. The presence of CTAB in this system would change the behavior of

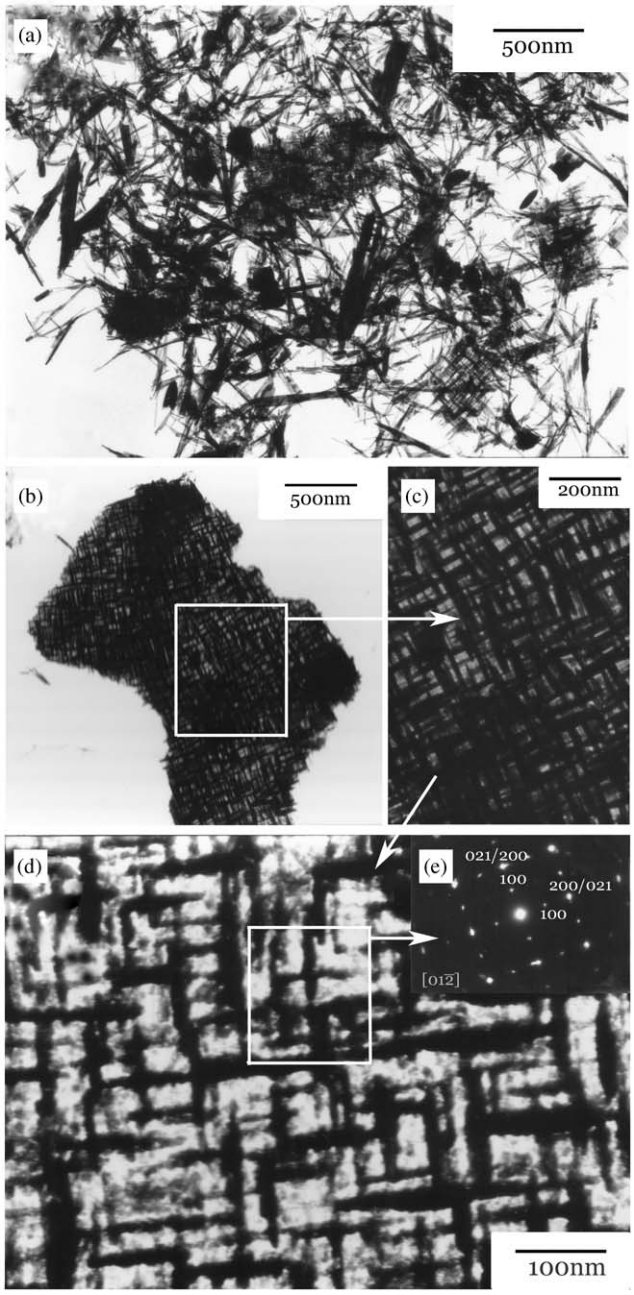

Fig. 4. (a) TEM image of nanofibers with several pieces of assembly structure; (b) a piece of well-organized assembly structure; (c) magnified image of (b); (d) detailed structure of a piece of network and its ED (e). Because of the long time exposure under electron beam, nanofibers in (d) have been eroded to a degree.

crystallization and orientation growth in one way, and consequently affect the morphologies of products. While taking into account the existence of self-assembly phenomena, the "orientated attachment" [27] mechanism probably also plays an important role in the system.

When $CdCl_2$ was dissolved in water with CTAB and Na_2WO_4, WO_4^{2-} preferred to combine with Cd^{2+} to form amorphous $CdWO_4$, and CTAB formed micelles in solution in the meanwhile. In this situation CTAB mainly has two effects. On one hand, micelles formed by CTAB enwrap the crystal nuclei and $CdWO_4$ amorphous particles that the crystallization process needs, and limit the crystallization in a relatively small circumscription and then inhibit crystal growth. On the other hand, CTA^+ cations can selectively adsorb on certain crystal planes of $CdWO_4$, and thereby decrease the surface energy and change the growth velocity of these planes.

In order to further investigate the effects of CTAB in this system, we carried out the reaction under different conditions such as different reaction time and different concentrations of CTAB. Fig. 5a shows the morphologies of samples that were reacted for 6 h. Besides rods with pointed ends, some spherical particles with pointed ends were also observed. We believe that these spherical particles are intermediates of the rods and further form the short nanorods through prolonging them along [100] direction. It is noticed that the diameters of these sphere particles are almost equal to the breadths of rods obtained by the reaction for 12 h. When the reaction time was extended to 24 h, the widths of these rods showed obvious change, which has been mentioned above (Figs. 2d and e). Thus, we conclude that extending the reaction time would mainly prolong the rods along the *a*-axis. Fig. 5b shows the morphologies of products obtained with half of the CTAB concentration compared with the typical procedure. Nanorods were obtained with thin nature and uniformity in size and aspect ratios, but without pointed ends. When the concentration of CTAB was twice as that of typical procedure, only very poorly defined thin sheet-like structures were found (data not shown here), while in the absence of CTAB, the obtained products were mainly rods without regular shape and size (Fig. 5c).

Based on the experiments discussed above, we assumed that CTA^+ cations would strongly bind to the (010) surface of $CdWO_4$ crystals and weakly bind to (100) and (001) faces, and then the surface energy of the (010) faces can be selectively lowered relative to that of (100) and (001) surfaces. The surface cleavage of $CdWO_4$ crystal also provides constructive information for explaining the adsorption of CTA^+ cations (Fig. 6). The zigzag orientations of W octahedral anions on (100) face results in this face becoming unfavorable for the adsorption of CTA^+ cations, whereas CTA^+ would prefer to adsorb on (010) face because of the high density of oxygen atoms on this face. In the typical procedure, the concentration of CTAB is very high and twice that of WO_4^{2-}. Thus there would be abundant CTA^+ in the system to adsorb on the (010) faces and even on (001) and (100) faces. Therefore, the surface energy of these faces would all be markedly reduced. Thus, it is possible to form a relatively thick nature along [010] direction. As we know, the more rapid the

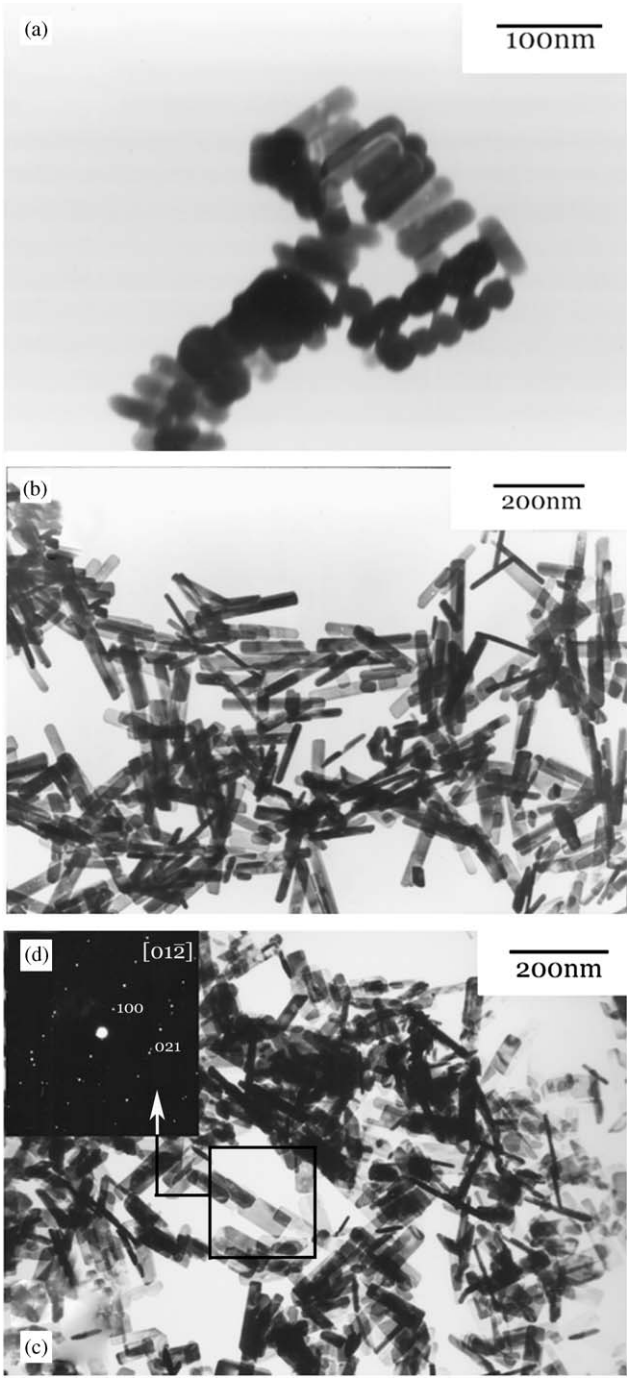

Fig. 5. TEM images of $CdWO_4$ nanorods obtained: (a) under typical procedure but with hydrothermal treatment for 6 h; (b) with half of CTAB concentration compared with typical procedure; (c) hydrothermal treatment for 12 h without CTAB and its ED (e).

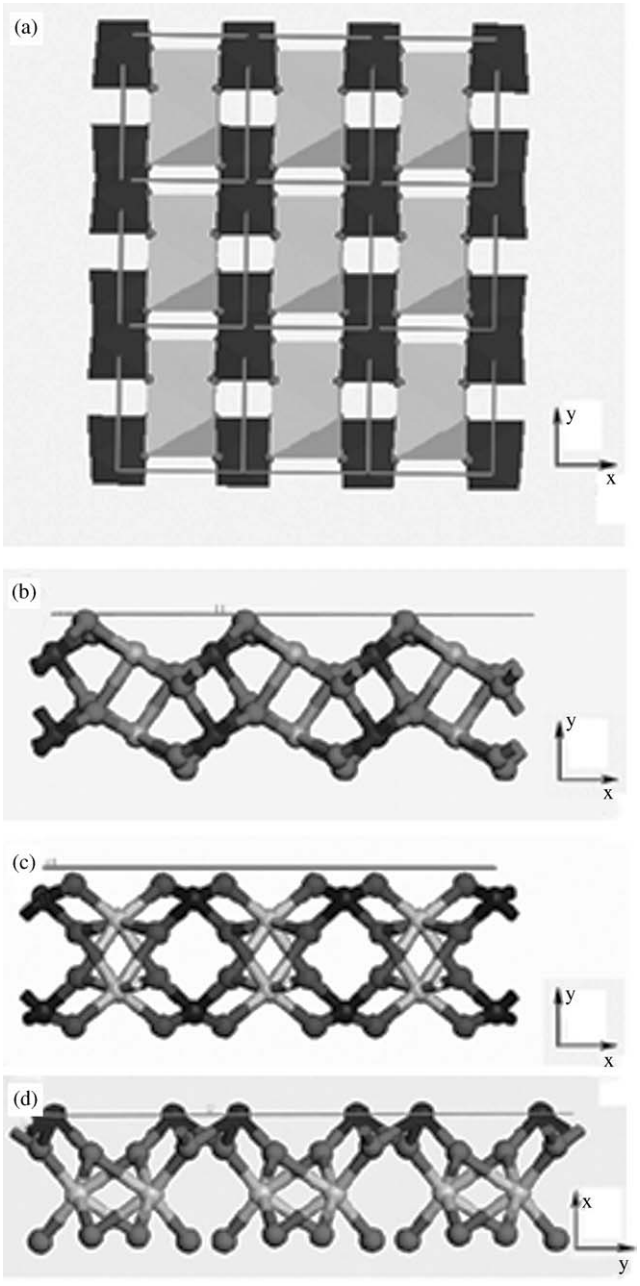

Fig. 6. The structure model illustration of $CdWO_4$ crystal ($3 \times 3 \times 3$ lattices). (a) *xy* projection; the surface structure cleavage of $CdWO_4$ crystal, (b) (001); (c) (010); (d) (100). The balls and octahedra of gray from deep to light denote W, O and Cd, representatively.

growth rate, the quicker the disappearance of a plane. Therefore, the (100) plane that has the most rapid growth rate almost disappears in the process, and results in the pointed shape in the ends of the rods (along *a*-axis). When the concentration of CTAB is reduced, more CTA^+ would preferentially adsorb on (010) faces because of the insufficiency of CTAB, which leads to the fastest growth rate along [100] directions and creates the thin nature in [010] direction. When the concentration of CTAB is excessively high, the product would be an irregular sheet-like structure because of the lamellar assembly formed by CTAB in the solution.

The self-assembly of short nanorods can be explicated from two aspects. First, according to the Onsager's theory, minimizing the excluded volume per particle in the array can maximize the entropy of the self-organized

structure and the higher sum of van der Waals forces along the nanorods' lengths compared with their tip that would lead these rods to preferrebly align parallelly [13,28,29], so the ordered structure strongly depended on the particle anisotropy. The second can be described as "oriented attachment" in which nanostructures can form larger structures via joining appropriate crystal faces, which has already been known in recent years [27] and some examples relative to this mechanism have been reported, such as TiO_2 [27,30,31], FeOOH [32], β-$Co(OH)_2$ [33], ZnS [34], ZnO [35] and $ZnWO_4$ [36]. Considering that the self-assembly has occurred in the early stage when the rods have not been maturely formed, we think that the "orientated attachment" mechanism would play a key role in the assembly process. In our current work, the assembly is only observed in the rods with pointed ends and most of the nanorods self-assembled using their (001) and (010) plane; so we suppose that the self-assembly has not been observed in lower CTAB concentration or without CTAB is partly due to the thin nature along [010] direction of these rods (Scheme 3).

It has been recently proved by Li et al. that CTAB and Na_2WO_4 can react under mild hydrothermal conditions to form mesolamellar ion pairs $[CTA]_2^{2+}[WO_4]^{2-}$ (CTA^+ = cetyltrimethylammonium cation) [37]. So it is possible to obtain $CdWO_4$ with different morphology through exact control of the reaction process, for example, $CdWO_4$ nanofibers can be obtained when CTAB and Na_2WO_4 were first dissolved in water and vigorously stirred to form a homogeneous solution, and then solid $CdCl_2$ was slowly added to the solution without stirring. In this process the viscosity of the reaction system is relatively high because of the comparatively high concentration of CTAB, and so the speed of $CdCl_2$ dissolving into the solution is slowed down considerably. Thus, Cd^{2+} in the system has a concentration grad at the beginning of the reaction and the amount of $CdWO_4$ crystal nuclei is also relatively less. At the same time, Cd^{2+} may also replace CTA^+ in $[CTA]_2^{2+}[WO_4]^{2-}$, which decelerates the production of nuclei and the growth of crystals as well, and makes the ionic species become precursors for further crystal growth. All the factors mentioned above

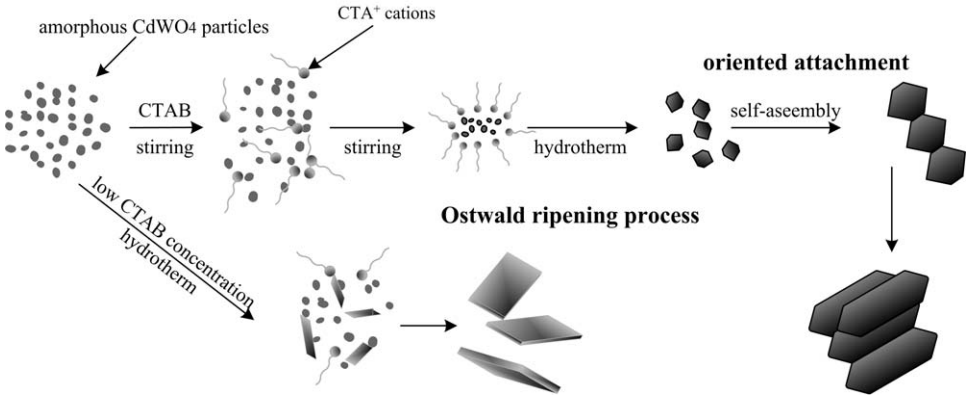

Scheme 3. Illustration of the growth and self-assembly of the nanorods.

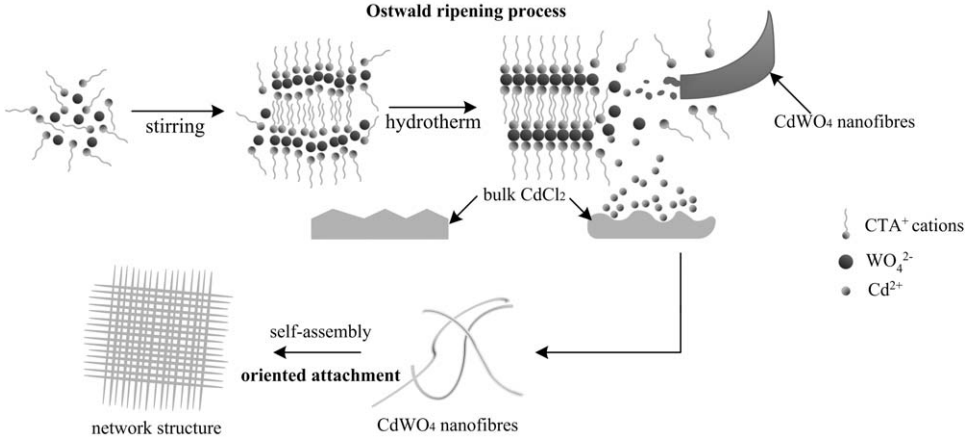

Scheme 4. Illustration of the growth and self-assembly of the nanofibers.

make $CdWO_4$ grow to relatively long nanofibers (Scheme 4). In the experimental process, tenuous nanofibers have been formed after 2 h (Fig. 7a), and with the increase in reaction time, nanofibers grow thick gradually. When the reaction time is up to 24 h, the nanofibers grow very long and attach together to form thicker fibers (Fig. 7b).

How these 1D nanofibers assemble to network structures is still under investigation. But we suppose that the certain crystal faces of nanofibers would prefer to attach together when they have the mutually perpendicular orientation during crystallization due to the specific structures of crystalline substrates, and the formation of these network structures may still primarily be caused by the "oriented attachment". From the experiment, we also found that the nanofibers also self-assembled to network structure in the early stage of synthesis.

Considering the discussion of the formation and assembly of nanorods and nanofibers, we think that the "Ostwald ripening process" and "oriented attachment" growth are two competitive mechanisms in the crystallization process. The former plays a key role in the formation and growth of the nanocrystals, while the latter determined the assembly of crystals.

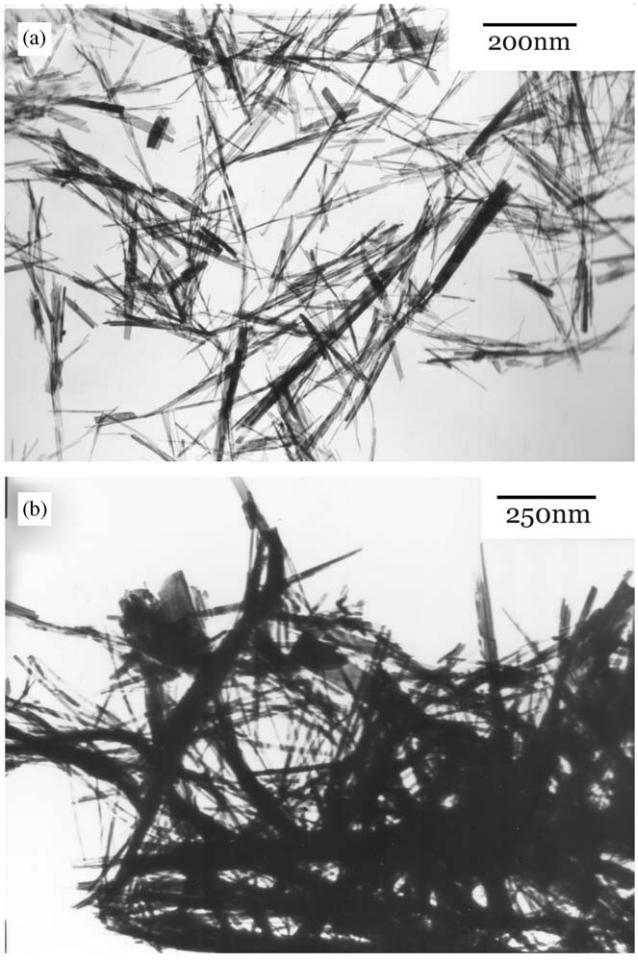

Fig. 7. TEM images of nanofiber obtained by typical procedure but with hydrothermal treatment for: (a) 2 h and (b) 24 h.

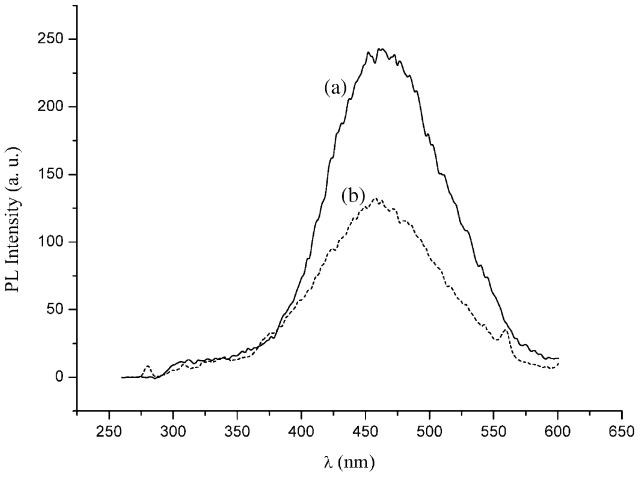

Fig. 8. Room temperature photoluminescence spectra: (a) nanorods and (b) nanofibers.

3.4. Photoluminescence property

The obtained $CdWO_4$ nanostructures exhibit a very strong blue emission band in the range 400–500 nm and the emission peaks are both at about 460 nm excited at 253 nm (Fig. 8), which well agrees with the PL emission of single cadmium tungstate crystal at room temperature but has a blue shift compared to what has been reported about "intrinsic luminescence" at 480–490 nm [16,38]. This PL emission is caused by the $^1A_1 \rightarrow {}^3T_1$ transitions within the WO_6^{6-} complex [39].

4. Conclusions

In summary, single crystalline $CdWO_4$ short nanorods and nanofibers can be selectively prepared based on hydrothermal treatment with CTAB as capping molecule from ordinary inorganic reactants. The crucial step in the process is whether there is stirring or not after $CdCl_2$ has been added to solution. With relatively thick nature along [010] direction, the obtained short nanorods have almost uniform breadth and pointed ends, which is different from the reported nanostructures of $CdWO_4$. And they can self-assemble together using their (001) and (010) faces to form an ordered structure, while nanofibers obtained in the procedure are flexible and can be arranged perpendicularly together to form a network structure like a woven intertexture. Both as-prepared nanorods and nanofibers display very strong blue-green luminescence property at room temperature. Further researches on the formation and self-assembly

mechanism of the nanorods and nanofibers are in progress.

Acknowledgment

This work is financially supported by the National Natural Foundation of China (50103006), the Shanghai Shu Guang Project (01-SG-15) and the Shanghai Nanomaterials Project (0241nm106).

References

[1] C.M. Lieber, Solid State Commun. 107 (1998) 607.
[2] J. Hu, T.W. Odom, C.M. Lieber, Acc. Chem. Res. 32 (1999) 435.
[3] C.N.R. Rao, A.K. Cheetham, J. Mater. Chem. 11 (2001) 2887.
[4] G.R. Patzke, F. Krumeich, R. Nesper, Angew. Chem., Int. Ed. 41 (2002) 2446.
[5] C.N.R. Rao, G.U. Kulkarni, P.J. Thomas, P.P. Edwards, Chem. -Eur. J. 8 (2002) 28.
[6] Y. Xia, P. Yang, Y. Sun, Y. Wu, B. Mayers, B. Gates, Y. Yin, F. Kim, H. Yan, Adv. Mater. 15 (2003) 353.
[7] H. Maeda, Y. Maeda, Langmuir 12 (1996) 1446.
[8] M. Li, H. Schnablegger, S. Mann, Nature 402 (1999) 393.
[9] F. Kim, S. Kwan, J. Akana, P.D. Yang, J. Am. Chem. Soc. 123 (2001) 4360.
[10] X. Peng, L. Manna, W. Yang, J. Wickham, E. Scher, A. Kadavanich, A.P. Alivisatos, Nature 404 (2000) 59.
[11] B.A. Korgel, D. Fitzmaurice, Adv. Mater. 10 (1998) 661.
[12] B.H. Hong, S.C. Bae, C.-W. Lee, S. Jeong, K.S. Kim, Science 294 (2001) 348.
[13] B. Nikoobakht, Z.L. Wang, M.A. El-Sayed, J. Phys. Chem. B 104 (2000) 8635.
[14] N. Saito, N. Sonoyama, T. Sakata, Bull. Chem. Soc. Japan 69 (1996) 2191.
[15] H. Lotem, Z. Burshtein, Opt. Lett. 12 (1987) 561.
[16] V.A. Pustovarov, A.L. Krymov, B. Shulgin, Rev. Sci. Instrum. 63 (1992) 3521.
[17] K. Tanaka, T. Miyajima, N. Shirai, Q. Zhang, R. Nakata, J. Appl. Phys. 77 (1995) 6581.
[18] K. Tanaka, D. Sonobe, Appl. Surf. Sci. 140 (1999) 138.
[19] Z.D. Lou, J.H. Hao, M. Cocivera, J. Lumin. 99 (2002) 349.
[20] K. Lennstrom, S.J. Limmer, G.Z. Cao, Thin Solid Films 434 (2003) 55.
[21] H.W. Liao, Y.F. Wang, X.M. Liu, Y.D. Li, Y.T. Qian, Chem. Mater. 12 (2000) 2819.
[22] S.H. Yu, M. Antonietti, H. Cöffen, M. Giersig, Angew. Chem., Int. Ed. 41 (2002) 2356.
[23] Y. Xiong, Y. Xie, Z. Li, X. Li, S. Gao, Chem. -Eur. J. 10 (2004) 654.
[24] C.J. Johnson, E. Dujardin, S.A. Davis, C.J. Murphy, S. Mann, J. Mater. Chem. 12 (2002) 1765.
[25] Y. Chang, H.C. Zeng, Cryst. Growth Des. 4 (2004) 397.
[26] J.W. Mullin, Crystallization, 2nd ed, Butterworth-Heinemann, London, UK, 1972.
[27] R.L. Penn, J.F. Banfield, Science 281 (1998) 969.
[28] J.C.P. Gabriel, P. Davidson, Top. Curr. Chem. 226 (2003) 119.
[29] N.R. Jana, Angew. Chem., Int. Ed. 43 (2004) 1536.
[30] A. Chemseddine, T. Moritz, Eur. J. Inorg. Chem. (1999) 235.
[31] R.L. Penn, J.F. Banfield, Geochim. Cosmochim. Acta 63 (1999) 1549.
[32] R.L. Penn, G. Oskam, T.J. Strathmann, P.C. Searson, A.T. Stone, D.R. Veblen, J. Phys. Chem. B 105 (2001) 2177.
[33] J.T. Sampanthar, H.C. Zeng, J. Am. Chem. Soc. 124 (2002) 6668.
[34] F. Huang, H.Z. Zhang, J.F. Banfield, Nano Lett. 3 (2003) 373.
[35] C. Pacholski, A. Kornowski, H. Weller, Angew. Chem., Int. Ed. 41 (2002) 1188.
[36] B. Liu, S.-H. Yu, L.J. Li, F. Zhang, Q. Zhang, M. Yoshimura, P.K. Shen, J. Phys. Chem. B 108 (2004) 2788.
[37] Y.D. Li, X.L. Li, R.R. He, J. Zhu, Z.X. Deng, J. Am. Chem. Soc. 124 (2002) 1411.
[38] M.M. Chirila, K.T. Stevens, H.J. Murphy, N.C. Giles, J. Phys. Chem. Solids 61 (2000) 675.
[39] K. Polak, M. Nikl, K. Nitsch, M. Kobayashi, M. Ishii, Y. Usuki, O. Jarolimek, J. Lumin. 72–74 (1997) 781.